COMPUTATIONAL MODELING OF HYDROGEN-ASSISTED FATIGUE CRACK GROWTH IN PIPELINE STEELS*

D. T. O'CONNOR
National Institute of Standards and Technology, Boulder CO, USA
B. E. LONG
Colorado School of Mines, Golden CO, USA
A. J. SLIFKA
National Institute of Standards and Technology, Golden CO, USA
E. S. DREXLER
National Institute of Standards and Technology, Boulder CO, USA
R. L. AMARO
Colorado School of Mines, Golden CO, USA

ABSTRACT

In this work we further develop a model to predict hydrogen-assisted fatigue crack growth in steel pipelines and pressure vessels. This model is implemented by finite element code, which uses an elastic-plastic constitutive model in conjunction with a hydrogen diffusion model to predict the deformation and concentration of hydrogen around a fatigue crack tip. The hydrogen concentration around the crack tip is used to inform our fatigue crack growth model and account for the effect of hydrogen embrittlement. We first use our model to predict the fatigue crack growth of X100 pipeline steel at different levels of applied hydrogen pressure. The simulated results are within a factor of ± 2 of the experimental X100 results.

INTRODUCTION

Hydrogen is expected to play a key role in transitioning the United States' energy and transportation sectors away from fossil fuels towards a more sustainable and climate-friendly alternative. While not an energy source, per se, hydrogen is seen as an energy carrier. In which case, hydrogen is used in conjunction with a catalyst to produce energy. Hydrogen may also be used to store energy from green energy-producing alternatives such as solar, wind, wave, and so on that produce energy regardless of demand. In order for hydrogen to see widespread use as an energy carrier, hydrogen must be safely and efficiently transported from the source to the location of end-use.

Hydrogen fuel cell vehicles are currently being manufactured and sold by Toyota, Hyundai, and Honda. Mercedes-Benz, Lexus, and Nissan have concept and evaluation vehicles currently in testing [1]. Unfortunately, there are currently only 29 hydrogen fueling stations in the United States [2]. The vast majority of those are in Northern and Southern California. The infrastructure required to transport hydrogen across the United States efficiently does not currently exist. Steel pipeline is thought to be the best method to transport

hydrogen long-distances. While the United States currently has on the order of 305,000 miles of natural gas pipeline [3] there is currently only approximately 700 miles to 1500 miles of hydrogen-dedicated pipeline for hydrogen delivery [4, 5]. A primary barrier to the use of steel pipeline to transport hydrogen is hydrogen's deleterious effects on steels monotonic and fatigue deformation response [6, 7]. The ASME B31.12 Committee on Hydrogen Piping and Pipelines is supporting the design, engineering, and installation of hydrogen-dedicated pipeline by creating and updating the B31.12 code based upon current hydrogen-assisted fatigue crack growth (HA-FCG) data collected at laboratories, such as the National Institute of Standards and Technology (NIST) and Sandia National Laboratories (SNL) [8-10] The data collected has been used to inform a phenomenological HA-FCG model for pipeline steels that predicts cycles to failure for known operating conditions. The model was based initially upon closed-form solutions for the crack-tip deformation response, the hydrogen diffusion within the material, and the coupling of the two [11, 12]. This work details the implementation of these key aspects of the HA-FCG model into the finite element code ABAQUS[1]. The results from the combination of deformation and hydrogen diffusion in ABAQUS are then coupled with the phenomenological HA-FCG model to predict the crack-growth response of X100 compact tension (CT) specimens tested in 1.72 MPa, 6.89 MPa, and 20.68 MPa gaseous hydrogen (250 psi, 1000 psi, and 3000 psi gaseous hydrogen).

Hydrogen-Assisted Fatigue Crack Growth Model

The existing phenomenological HA-FCG model, calibrated to X100 pipeline steel, is detailed in [11, 12]. The form of the model is as follows:

$$\frac{da}{dN_{\text{total}}} = \frac{da}{dN_{\text{fatigue}}} + \delta\left(P_{\text{H}} - P_{\text{H}_{\text{th}}}\right)\frac{da}{dN_{\text{H}}}, \qquad \text{EQ. 1}$$

where, a is the crack length, N is the number of cycles, and P is the hydrogen pressure. From left to right, the total fatigue crack growth is calculated as a summation of the fatigue crack growth resulting from fatigue only and the hydrogen-assisted fatigue crack growth. The HA-FCG term has the form:

$$\frac{da}{dN_{\text{H}}} = \left[\left(\frac{da}{dN_{P_{\text{H}}}}\right)^{-1} + \left(\frac{da}{dN_{\Delta K}}\right)^{-1}\right]^{-1}, \qquad \text{EQ. 2}$$

where the overall contribution of HA-FCG is modeled as a competition between a hydrogen-pressure-dominated component, $\frac{da}{dN_{P_{\text{H}}}}$, and a component dominated by hydrogen-assistance from the crack-extension driving force , $\frac{da}{dN_{\Delta K}}$. This competition is a result of two independent damage mechanisms. When the crack extension per cycle is on the order of the fatigue process zone (FPZ) size, the crack growth rate is dominated by the accumulated damage of the FPZ and the increased hydrogen concentration within the FPZ. However, when the crack extension per cycle extends far beyond the FPZ, P_{H}, the crack growth rate is dominated less by the effects within the FPZ and more by the far-field crack driving force, ΔK. The hydrogen-pressure-dominated FCG term is defined as

[1] Identified for clarity only, no endorsement by NIST is implied

$$\frac{da}{dN_{P_H}} = a1\Delta K^{B1}\left(P_H^{m1} exp^{\left(\frac{-Q+V\sigma_h}{RT}\right)}\right)^{d1}, \quad \text{EQ. 3}$$

and is referred to as transient HA-FCG, where ΔK is the stress intensity range, Q is the activation energy for hydrogen diffusion; V is the partial molar volume of hydrogen in the metal; R is the universal gas constant; T the absolute temperature; σ_h is the hydrostatic stress at a critical distance in front of the crack tip; P_H is the ambient hydrogen pressure; and *a1*, *B1*, *m1*, and *d1* are fitting parameters. The component dominated by hydrogen-assistance from the crack-extension driving force is defined as

$$\frac{da}{dN_{\Delta K}} = a2\Delta K^{B2}\left(P_H^{m2} exp^{\left(\frac{-Q+V\sigma_h}{RT}\right)}\right)^{d2}, \quad \text{EQ. 4}$$

and is referred to as the steady-state HA-FCG, where *a2*, *B2*, *m2*, and *d2* are fitting parameters. Explicit details of the model justification, constants, parameters, calibration, etc. may be found in [11]. One will note that Eqs. 3 and 4 employ closed-form solutions for the stress-free hydrogen concentration within the material, P_H^{m2}, the stress field at a crack tip, σ_h, and the stress-assisted hydrogen concentration near the crack tip, $P_H^{m2} exp^{\left(\frac{-Q+V\sigma_h}{RT}\right)}$.

ABAQUS Implementation

Ultimately, the HA-FCG model defined above is to be implemented in a physics-based format that predicts the FCG, based upon microstructure-specific material responses, such as hydrogen diffusivity, hydrogen-dislocation interactions, microstructure-specific deformation, etc. A first step towards this aim is to determine the stress-free and stress-assisted hydrogen concentration within the material, both near the crack tip and far field, by use of the finite element code ABAQUS. For this purpose, Eq. 3 is then replaced by

$$\frac{da}{dN_{P_H}} = a1\Delta K^{B1}(C_L)^{d1}, \quad \text{EQ. 5}$$

where C_L is the spatial- and time-dependent lattice hydrogen concentration determined from ABAQUS (defined in EQ. 10 below). Equation 4 is also replaced with

$$\frac{da}{dN_{\Delta K}} = a2\Delta K^{B2}(C_L)^{d2}, \quad \text{EQ. 6}$$

and *a2*, *B2*, *m2*, and *d2* are fitting parameters [12].

The finite-element implementation to determine C_L requires an understanding of the elastic-plastic deformation response of the material. This modeling effort employs the Ramberg-Osgood (RO) elastic-plastic constitutive model

$$\frac{\varepsilon}{\varepsilon_0} = \frac{\sigma}{\sigma_0} + \alpha\left(\frac{\sigma}{\sigma_0}\right)^n, \quad \text{EQ. 7}$$

where ε is the total strain, σ is the total stress, ε_0 and σ_0 are the strain and stress at yielding, respectively, and α and n are constants. The Ramberg-Osgood deformation model is implemented in ABAQUS with the existing cyclic plasticity model incorporating linear kinematic hardening.

Hydrogen transport is modeled in ABAQUS by use of a new user-defined subroutine, H-diff, which is built upon the structure of the existing ABAQUS

subroutine UMATHT. The subroutine H-diff explicitly calculates the hydrogen concentration, C_L, the plastic-hardening curve, and the hydrostatic stress by use of EQ. 7 at the integration points as a function of time. The hydrogen concentration is calculated via the hydrogen transport equation of [13] and modified by [14]

$$\frac{D}{D_{\text{eff}}}\frac{\partial C_L}{\partial t} = D\nabla^2 C_{\text{L}} - \nabla\cdot\left(\frac{DV_{\text{H}}}{3RT}C_{\text{L}}\nabla\sigma_{\text{h}}\right) - \left(\sum_j \eta^j \theta_{\text{T}}^j \frac{\partial N_{\text{T}}^j}{\partial \varepsilon^{\text{p}}}\right)\frac{\partial \varepsilon^{\text{p}}}{\partial t}. \qquad \text{EQ. 8}$$

The variables in Eq. 8 are as follows: D is the hydrogen diffusion coefficient, D_{eff} is the effective diffusion coefficient, C_{L} is the hydrogen concentration in the normal interstitial lattice site (NILS), V_{H} is the partial molar volume of hydrogen, R is the universal gas constant, T is the absolute temperature, σ_{h} is the hydrostatic stress, η is the number of trapping sites per trap type j, θ_{T} is the trap site occupancy for a given trap site j, N_{T} is the trap-site density for a given trap site j, ε^{p} is the equivalent plastic strain and the ∇ is the mathematical vector differential operator. Equation 8 is an extension of Fick's law that incorporates the influence of both hydrostatic stress and plastic strain on hydrogen transport. While Eq. 8 may be used for three types of traps, i.e. carbides, grain boundaries and dislocations, this model implementation is only concerned with the so-called weak traps. In this case, Eq. 8 is used to model hydrogen diffusion resulting only from NILS and dislocations. Oriani's theory [15] provides the relationship between the trap-site occupancies, θ_{T}^j, and the lattice-site occupancies, θ_L, as

$$\frac{\theta_{\text{T}}^j}{1-\theta_{\text{T}}^j} = \frac{\theta_{\text{L}}}{1-\theta_{\text{L}}} exp\left(\frac{W_{\text{B}}^j}{RT}\right), \qquad \text{EQ. 9}$$

where W_{B}^j is the trap binding energy for the trap of interest, dislocations in this case. The hydrogen concentration in the NILS and the trap sites is given by EQ. 10 and EQ. 11, respectively.

$$C_{\text{L}} = \beta N_{\text{L}}\theta_{\text{L}} \qquad \text{EQ. 10}$$

$$C_{\text{T}}^j = \eta^j N_{\text{T}}^j \theta_{\text{T}}^j \qquad \text{EQ. 11}$$

Literature values are used for the number of interstitial sites per atom, β, the number of solvent atoms per unit volume, N_{L}, and the number of trap sites per trap type, η^j. The trap densities for a given trap type, N_{T}^j, taken here as the trap density for only dislocations, is solved as a function of equivalent plastic strain, per the work of [16]. The relationship is given in EQ. 12

$$N_{\text{T}}^{\text{dislocations}} = \frac{10^{23.26-2.33exp(-5.5\varepsilon^p)}}{N_A}, \qquad \text{EQ. 12}$$

where N_A is Avogadro's constant. Finally, the effective hydrogen diffusion is calculated by use of

$$\frac{D}{D_{\text{eff}}} = 1 + \sum_j \frac{\partial C_{\text{T}}^j}{\partial C_{\text{L}}}. \qquad \text{EQ 13.}$$

Equations 8 through 13 are solved for each integration point at each time step within the new user-defined material model H-Diff.

HA-FCG Calibration to an API-5L X100 Pipeline Steel

An API-5L X100 pipeline steel has been characterized at NIST and was used as the model material for the original HA-FCG implementation [11]. HA-FCG tests were conducted on compact tension specimens in the transverse-

longitudinal (TL) orientation at a load ratio of R=0.5 (were R=K_{min}/K_{max} in this case) in various hydrogen pressures. The material's chemical composition is provided in Table 1. The material's microstructure is shown in Fig. 1a and can be characterized by having an average grain size on the order of 1 micron.

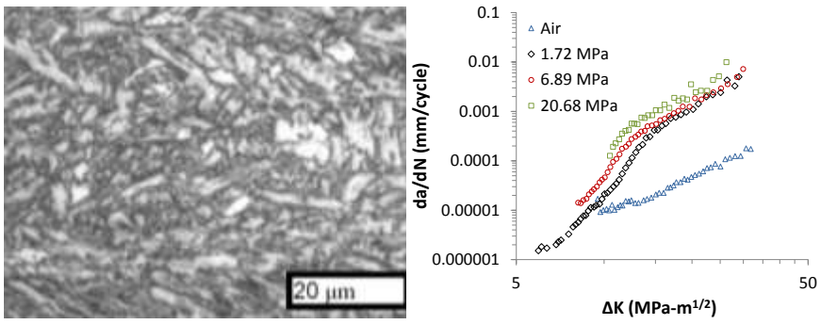

(a) **(b)**

Figure 1: (a) Image of X100 microstructure, (b) HA-FCG of X100 steel as a function of environment, R=0.5.

The monotonic test results for this material, Ramberg-Osgood fit parameters, as a function of air and varying hydrogen pressures, along with its HA-FCG response are detailed in [11, 12] and provided here for completeness. Full experimental details for collection of the data in Table 2 and Figure 1b are provided in [11, 17].

Table 1: Chemical composition of API steels tested, mass %.

	Al	C	Co	Cr	Cu	Fe	Mn	Mo
X100	0.012	0.064	0.003	0.023	0.28	96.90	1.87	0.23

	N	Nb	Ni	P	Si	Ti	V
X100	0.003	0.017	0.47	0.009	0.099	0.017	0.002

Table 2: Monotonic test results and R-O fitting parameters for X100 [12].

	H_2 Pressure	σ_0	ε_0	n	α	E
Material	MPa	MPa	-	-	-	GPa
X100	AIR	693.01	0.0032	13.48	0.92	214.14
Longitudinal	5.5	700.37	0.0032	13.39	1.01	219.17
	13.8	700.90	0.0032	13.78	1.11	218.89
	27.6	708.86	0.0031	13.56	1.03	229.61
	68.9	714.01	0.0033	14.34	0.97	215.74
X100	AIR	804.47	0.0035	17.18	2.97	229.58
Transverse	13.8	810.23	0.0035	15.33	3.52	230.52
X52	AIR	442.21	0.0021	11.74	3.10	212.42

One will note from Table 2 that for a given orientation with respect to the rolling direction (longitudinal or transverse), the X100 tested has relatively stable yielding and post-yielding response as a function of environment, as indicated by the R-O parameters. Perhaps not surprising given the microstructural texture shown in Fig. 1a, the material exhibits noticeable orientation anisotropy in both

its yielding and post-yielding behavior. Figure 1b depicts the FCG results of the X100 in both air and high-pressure hydrogen. Figure 1b indicates that the X100 material tested is susceptible to changes in hydrogen pressure, with increased FCG rates at higher pressures.

To determine the hydrogen lattice concentration, C_L, a one-half symmetry CT specimen was modeled in ABAQUS and is shown in Fig. 2a. The symmetry plane was created along the presumed crack path at the geometric center line. Given that the CT specimens were tested in the TL orientation, the X100 material properties from the transverse orientation were used in this study. Specimens having various crack lengths were created. The crack lengths and applied loads were calculated by use of ASTM E647 to ensure resulting ΔK values of 7 MPa-m$^{0.5}$, 9 MPa-m$^{0.5}$, 11 MPa-m$^{0.5}$, 13 MPa-m$^{0.5}$, and 15 MPa-m$^{0.5}$. Simulations were then run at the five ΔK values for air, and hydrogen gas pressures of 1.72 MPa, 6.89 MPa, and 20.68 MPa. The ambient hydrogen pressure was implemented in ABAQUS by way of the calculated chemical potential. The full model parameters required for the hydrogen diffusion study in ABAQUS are taken from [14] and are given in Table 3. Figure 2b provides the resulting imagery of the lattice hydrogen concentration at a crack tip of a CT specimen experiencing ΔK=15 MPa-m$^{0.5}$ in 6.89 MPa gaseous hydrogen.

Table 3: Hydrogen diffusion material parameters.

D (m^2/s)	V_H (m^3/mol)	N_L (mol/m^3)	W_B (J/mol)	β	η
1.28×10^{-8}	2.0×10^{-6}	8.46×10^{-28}	6.1×10^{4}	1	1

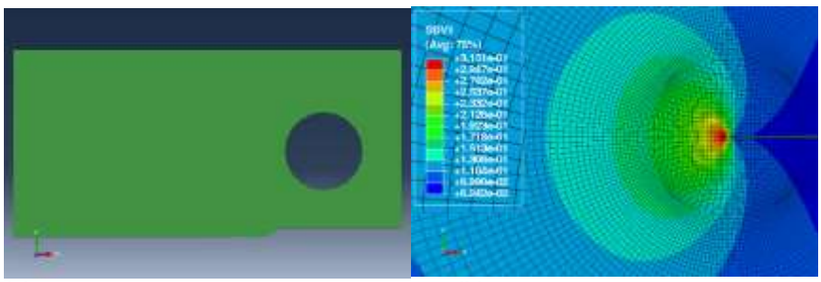

(a) **(b)**

Figure 2: (a) Symmetry CT specimen geometry; (b) Predicted hydrogen concetration at the crack tip for ΔK=15 MPa-m$^{0.5}$, R=0.5, and a hydrogen pressure of 6.89 MPa.

Although no data currently exists to calibrate the lattice hydrogen concentration, the results provided in Fig. 2b are as expected [13]. The predicted fatigue crack growth for the twenty combinations of ΔK and environments of interest were calculated by use of the lattice hydrogen concentrations predicted from ABAQUS in conjunction with Eqs. 5 and 6. The FCG predictions are shown with the experimental data in Fig. 3. The results depicted in Fig. 3 indicate that the model implementation performs very well at predicting the HA-FCG for a

CT-specimen of X100 for varying ΔK and hydrogen pressures with predicted values within a factor of ± 2 of the experimental results.

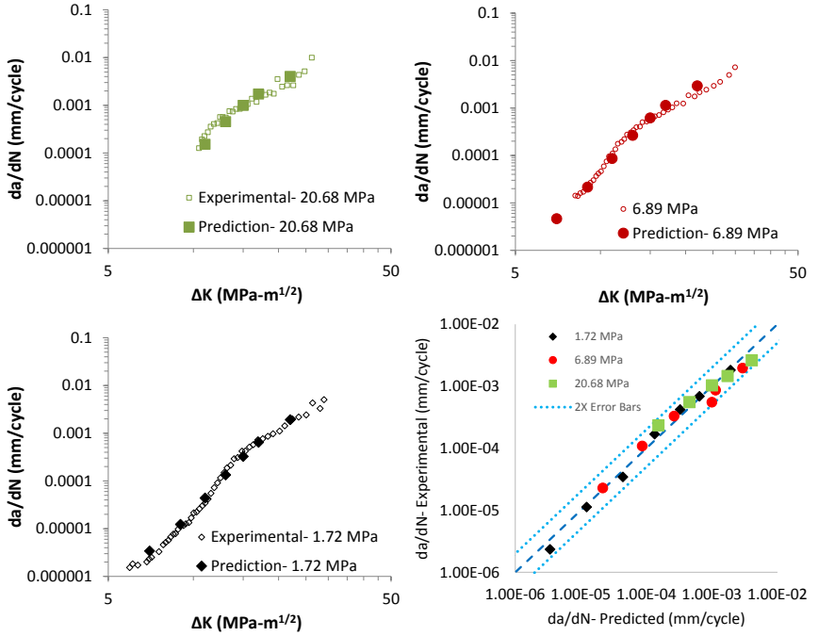

Figure 3: Experimental and predicted HA-FCG for an X100 steel at various pressures of hydroegn gas.

CONCLUSIONS

A new ABAQUS user-defined material model for stress- and plastic strain-assisted hydrogen diffusion, has been created by use of the existing ABAQUS UMATHT. The new hydrogen diffusion model has been coupled with the elastic-plastic material response to predict predict hydrogen-free deformation, deformation in the presence of hydrogen, and the lattice hydrogen concentration of an API-5L X100 material. Furthermore, the physics-based model, which combines deformation and the hydrogen diffusion, has been coupled with an existing phenomenological HA-FCG model. The modeling results accurately predict HA-FCG within a factor of ± 2.

REFERENCES

1. *U.S. Depratment of Energy, Energy Eficiency & Renewable Energy, Fuel Cell Links- Vehicles and Manufacturers*. 2016 7/24/2016]; Available from: www.fueleconomy.gov/feg/fcv_links.shtml.
2. *U.S. Depratment of Energy, Energy Eficiency & Renewable Energy, Alternative Fuels Data Center- Alternative Fueling Station Locator*. 2016 7/24/2016]; Available from: www.afdc.energy.gov/locator/stations/.

3. *United States Energy Information Administration, About U.S. Natural Gas Pipelines*. 2016 7/24/2016]; Available from: www.eia.gov/pub/oil_gas/natural_gas/analysis_publications/ngpipeline/index.html.
4. *U.S. Depratment of Energy, Energy Eficiency & Renewable Energy, Alternative Fuels Data Center, Hydrogen Production and Distribution*. 2016 7/24/2016]; Available from: www.afdc.energy.gov/fuels/hydrogen_production.html#distribution.
5. *U.S. Office of Energy Efficiency & Renewable Energy, ENERGY.gov, Hydrogen Pipelines*. 2016; Available from: http://energy.gov/eere/fuelcells/hydrogen-pipelines.
6. Somerday, B., P., *Technical Reference on Hydrogen Compatibility of Materials- Plain Carbon Ferritic Steels: C-Mn Alloys (Code 1100)*, 2008, Sandia National Laboratories, Livermore, CA. p. 32.
7. Nanninga, N.E., Levy, Y. S., Drexler, E. S., Condon, R. T., Stevenson, A. E., Slifka, A. J., *Comparison of hydrogen embrittlement in three pipeline steels in high pressure gaseous hydrogen environments.* Corrosion Science, 2012. **59**(0): p. 1-9.
8. Slifka, A.J., Drexler, E. S., Nanninga, N. E., Levy, Y. S., McColskey, J. D., Amaro, R. L., Stevenson, A. E., *Fatigue crack growth of two pipeline steels in a pressurized hydrogen environment.* Corrosion Science, 2014. **78**(0): p. 313-321.
9. Drexler, E.S., Slifka, A. J., Amaro, R. L., Barbosa, N., Lauria, D. S., Hayden, L. E., Stalheim, D. G., *Fatigue crack growth rates of API X70 pipeline steel in a pressurized hydrogen gas environment.* Fatigue & Fracture of Engineering Materials & Structures, 2014. **37**(5): p. 517-525.
10. San Marchi, C., Somerday, B. P., Nibur, K. A., Stalheim, D. G., Boggess, T., Jansto, S., *Fracture and Fatigue of Commercial Grade API Pipeline Steels in Gaseous Hydrogen*, in *ASEM 2010 Pressure Vesselss and Piping Conference*2010: Bellevue, WA, USA.
11. Amaro, R.L., Rustagi, N., Findley, K. O., Drexler, E. S., Slifka, A. J., *Modeling the fatigue crack growth of X100 pipeline steel in gaseous hydrogen.* International Journal of Fatigue, 2014. **59**(0): p. 262-271.
12. Amaro, R.L., Drexler, E. S., Slifka, A.J., *Fatigue crack growth modeling of pipeline steels in high pressure gaseous hydrogen.* International Journal of Fatigue, 2014. **62**(0): p. 249-257.
13. Sofronis, P., McMeeking, R. M., *Numerical analysis of hydrogen transport near a blunting crack tip.* Journal of the Mechanics and Physics of Solids, 1989. **37**(3): p. 317-350.
14. Novak, P., Yuan, R., Somerday, B. P., Sofronis, P., Ritchie, R. O., *A statistical, physical-based, micro-mechanical model of hydrogen-induced intergranular fracture in steel.* Journal of the Mechanics and Physics of Solids, 2010. **58**(2): p. 206-226.
15. Oriani, R.A., *The diffusion and trapping of hydrogen in steel.* Acta Metallurgica, 1970. **18**(1): p. 147-157.
16. Kumnick, A.J., Johnson, H. H., *Deep trapping states for hydrogen in deformed iron.* Acta Metallurgica, 1980. **28**(1): p. 33-39.
17. Nanninga, N.E., Levy, Y. S., Drexler, E. S., Condon, R. T., Stevenson, A. E., Slifka, A. J., *Comparison of hydrogen embrittlement in three pipeline steels in high pressure gaseous hydrogen environments.* Corrosion Science, 2012. **59**: p. 1-9.

Materials Performance in Hydrogen Environments

Proceedings of the 2016

International Hydrogen Conference

September 11-14, 2016

Jackson Lake Lodge, Wyoming, USA

Edited by

B.P. Somerday

P. Sofronis

ISBN: 978-0-7918-6138-7
ASME Book Number: 861387